Acta Materialia 142 (2018) 193–200

Contents lists available at ScienceDirect

Acta Materialia

journal homepage: www.elsevier.com/locate/actamat

Full length article

On the characterisation of antisite defects and ordering in off-stoichiometric Fe_2VAl-based Heusler compounds by X-ray anomalous diffraction

Camille van der Rest [a], Alain Schmitz [b], Pascal J. Jacques [a, *]

[a] Université catholique de Louvain (UCL), Institute of Mechanics, Materials and Civil Engineering, IMAP, Place Sainte Barbe 2 Bte L5.02.02, 1348 Louvain-la-Neuve, Belgium
[b] CRM Group, Avenue Du Bois Saint-Jean 21, B27–Quartier Polytech 4, 4000 Liège, Belgium

ARTICLE INFO

Article history:
Received 14 March 2017
Received in revised form
6 September 2017
Accepted 12 September 2017
Available online 14 September 2017

Keywords:
Heusler alloys
Order–disorder phenomena
X-ray diffraction (XRD)
Anomalous scattering
Neutron diffraction

ABSTRACT

Compounds based on Fe_2VAl are good candidates for low grade heat harvesting owing to the thermoelectric effect. However, it is claimed that their thermoelectric properties are badly influenced by antisite defects, especially at higher temperatures. The present study investigates order-disorder transitions in Fe_2VAl ternary Heusler compounds. An inherent problem of these compounds is the close atomic numbers of Fe and V, leading to similar x-ray atomic scattering factors. Hence, the $D0_3$ and $L2_1$ structures, corresponding to Fe-V antisite defects, are hardly distinguishable by X-ray diffraction. In this work, anomalous scattering and neutron diffraction were successfully combined with differential scanning calorimetry to highlight the order-disorder transitions in Fe_2VAl-based compounds. A model has been developed to quantify the ordering parameters. From these results, specific heat-treatments were defined to promote the formation of the $L2_1$ ordered phase.

1. Introduction and background

Heusler alloys are the topic of numerous recent studies due to promising functional properties in various fields [1–3]. This is also the case for the Fe_2VAl compound that was shown to exhibit very interesting thermoelectric properties adequate for low grade heat harvesting [4–8]. Like other Heusler compounds of general formula X_2YZ (where X and Y are transition metals and Z is a main group element), the Fe_2VAl-based compound belongs to the cubic space group (Fm-3m) with four interpenetrating FCC sublattices. In a fully ordered configuration, two of these sublattices are occupied by X atoms, and the two other ones are occupied by Y and Z atoms, respectively. X atoms (Fe in the present case) occupy tetrahedral sites referred to as the 8(c) Wyckoff positions, while the Y and Z atoms (V and Al) occupy the octahedral 4(a) and 4(b) Wyckoff positions [1]. The resulting structure is the fully ordered Heusler structure, referred to as the $L2_1$ crystal structure and shown on Fig. 1. Perfect $L2_1$ order could be only partially present depending on the processing conditions. The crystal structure is then described more adequately using lower-ordered structures. If the V and Al atoms are randomly distributed, the 4(a) and 4(b) Wyckoff sites become equivalent, bringing B2-type disorder. As a consequence, the symmetry is reduced and the space group becomes Pm-3m [1]. If, on the other hand, V and Fe atoms interchange such that their distribution over the 8(c) and 4(a) sites is random, $D0_3$-type disorder is observed. It may be noted that this is the crystal structure of Fe_3Al (same space group Fm-3m). Finally, the A2-type structure arises in the case of completely random distribution of atoms. This disordered structure results in a BCC lattice which belongs to the Im-3m space group.

Bilc et al. [9] have shown that Fe-V antisite defects are the most detrimental antisite defects for the thermoelectric properties of Fe_2VAl-based compounds. It emphasises the importance of accurately characterising the degree of order of such Heusler compounds.

Powder X-ray diffraction (XRD) has been commonly used as experimental method to determine the crystal structure of Heusler samples [1,10]. The presence of the (111) superlattice reflection is sometimes considered in the literature as an evidence for the $L2_1$ structure [7]. Other authors calculate intensity ratios to identify the $L2_1$ structure, without making a clear distinction with the $D0_3$ phase [11,12]. However, it is recognised that powder X-ray

* Corresponding author.
E-mail address: pascal.jacques@uclouvain.be (P.J. Jacques).

https://doi.org/10.1016/j.actamat.2017.09.024
1359-6454/

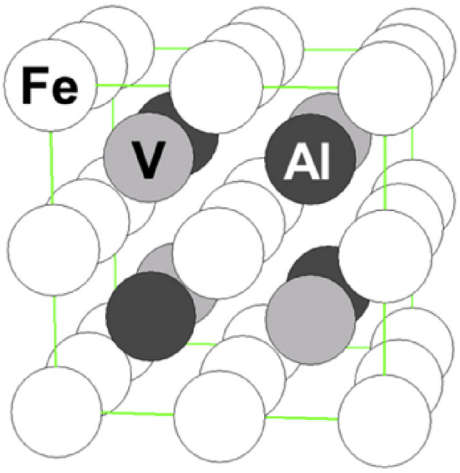

Fig. 1. Visualisation of the fully ordered $L2_1$ structure, so-called Heusler structure.

diffraction presents difficulties in discriminating some structures and identifying antisite disorder between elements with close atomic numbers, such as Fe and V [10]. Indeed, the X-ray diffracted intensities are proportional to the atomic numbers of the constitutive elements when X-ray source wavelength does not induce sample fluorescence (normal scattering). To overcome this drawback, anomalous XRD analysis could be helpful to properly determine the structure [1,13,14].

In XRD, the structure factor F_{hkl} characterises the wave diffracted by the different atoms of the unit cell for a (hkl) reflection and is used, among other factors (multiplicity, Lorentz-polarisation, temperature, and absorption), to determine the diffracted intensities [13,15]. Equation (1) shows the general expression of the diffracted intensity in XRD relating the diffracted intensity I_{hkl} to $|F_{hkl}|^2$, which is calculated by multiplying F_{hkl} by its complex conjugate [16]. In Equation (1), p_{hkl} is the multiplicity factor; LP factor is the Lorentz-polarisation factor resulting from geometrical considerations and from the fact that the incident beam is unpolarised; T factor is the temperature factor that takes into account thermal vibrations of the atoms[1] [15,17]. The absorption factor is independent of θ in the present configuration so that it does not influence relative intensities.

$$I_{hkl} \propto |F_{hkl}|^2 \cdot p_{hkl} \cdot \underbrace{\left(\frac{1+\cos^2 2\theta}{\sin^2\theta\cos\theta}\right)}_{\text{LP factor}} \cdot \underbrace{exp\left(-2B\left(\frac{\sin\theta}{\lambda}\right)^2\right)}_{\text{T factor}} \quad (1)$$

The structure factor F_{hkl}, for a (hkl) reflection and for a unit cell containing N atoms, is calculated as a function of the atomic scattering factors $f_1, \ldots, f_N$ by Equation (2) [13,16]. The structure factors are thus dependent on the position (u_n, v_n, w_n are the atomic coordinates) and nature of the atoms in the unit cell, hence on (dis) order.

$$F_{hkl} = \sum_{n=1}^{N} f_n e^{2\pi i(hu_n + kv_n + lw_n)} \quad (2)$$

The normal atomic scattering factors $f_{at} = f_0$ are commonly used when no fluorescence is taking place. These ones are nearly proportional to the atomic number Z_{at}, hence very similar for atoms like Fe and V. In the case of fluorescence, correction factors have to be added to describe more accurately the scattering of atoms. Equation (3) shows that the atomic scattering factors do include a complex energy-dependent contribution, $f' + if''$, referred to as the anomalous correction factors [13]. In this equation, f_0 is the normal contribution dependent on the centrosymmetry of the electron distribution and decreasing rapidly when increasing $\sin\theta/\lambda$, θ referring to the direction of observation and λ to the wavelength of the incident radiation.

$$f(\lambda,\theta) = f_0\left(\frac{\sin\theta}{\lambda}\right) + f'(\lambda) + if''(\lambda) \quad (3)$$

The anomalous contributions are most of the time insignificant in comparison to f_0, except in the vicinity of an absorption edge when core electrons can be excited by incident photons [13,17]. Fig. 2 shows, for Fe and V, the strong dependence of the anomalous contributions f′ and f″ on energy, with large variations near absorption edges (5.4651 keV for V and 7.112 keV for Fe) [18]. By choosing incident X-ray with energy near the Fe or V absorption edges, the atomic scattering factors of these two atoms can be much more different so that it would be possible to identify with a larger contrast their positions in the lattice (and thus potentially Fe-V antisite disorder) [13].

2. Model for the identification and quantification of disorder in Fe_2VAl

2.1. Previous models

Takamura et al. suggested a model, based on anomalous XRD, which evaluates three disordering parameters (α, β, and γ) to characterise ordering in the Co_2FeSi Heusler compound [10]. Three types of antisite exchanges are considered: Fe/Si, Co/Si, and Co/Fe exchanges, whose numbers per unit formula correspond to the three disordering parameters, respectively. From experimental values of $|F_{111}|^2/|F_{220}|^2$ and $|F_{200}|^2/|F_{220}|^2$, obtained from XRD with Co and Cu sources, i.e. with different levels of anomalous

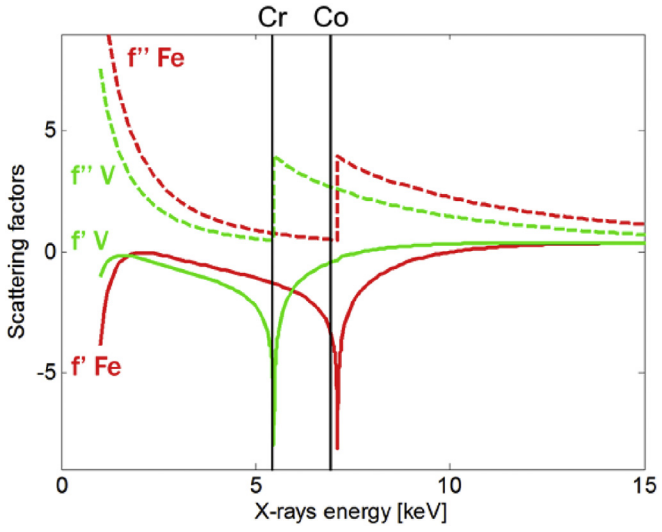

Fig. 2. Anomalous contribution to the atomic scattering factors of Fe (in red) and V (in green): $f = f_0 + f' + if''$. This energy-dependent contribution has a real part f′ (solid lines) and an imaginary part f″ (dashed lines). The X-ray energies of Cr and Co (Kα1) sources used in this work are highlighted (Inspired by Merritt [18].). (For interpretation of the references to colour in this figure legend, the reader is referred to the web version of this article.)

[1] In the $L2_1$ structure, p = 8, 6, and 12 for the (111), (200), and (220) plane families, respectively. Based on the literature, the B parameter of the temperature factor is set at 0.9 [12].

scattering, they got four ratios of experimental structure factors used as input for the model then solved by a least square refinement method to find α, β, and γ, respectively [10]. On the other hand, Umetsu et al. developed a model, based on neutron diffraction, to characterise the degree of $L2_1$ order in Co_2YGa compounds (Y = Ti, V, Cr, Mn, Fe) [19]. Indeed, neutron diffraction allows to discriminate between neighbouring elements in the periodic table, such as transition metals between Ti and Co, since the scattering length b_0 (equivalent to the atomic scattering factor for XRD) is no longer proportional to the atomic number Z_{at} [20]. They defined the atomic fractions p_i^j of atom i on site j of the crystal structure, giving nine quantities related by five independent relations (conditions on the sum of each atom and of each site, see Equation (4)), leading ultimately to four free variables [19]. However, they claimed that neutron diffraction gives only two kinds of information from the 111- and the 200-type superlattice reflections. Based on results on the binary CoGa alloy, they assumed that no exchange occurs between Co and Ga (no A2 structure) and they thus kept two unknown parameters p_{Co}^{X} and p_{Ga}^{Z} found by the Rietveld method [19].

$$\begin{aligned} &\forall i, p_{j1}\, p_i^{j1} + p_{j2}\, p_i^{j2} + p_{j3}\, p_i^{j3} = c_i \\ &\forall j, p_{i1}^{j} + p_{i2}^{j} + p_{i3}^{j} = 1 \end{aligned} \tag{4}$$

Both above-mentioned models present a strong limitation since they consider only strictly stoichiometric compounds [10,19]. Based on these previous models, it is proposed here to quantify all kinds of (dis)order: $L2_1$, $D0_3$, B2, and A2 owing to anomalous XRD (Co and Cr sources), while considering off-stoichiometry. Indeed, some off-stoichiometric Heusler compounds present interesting properties. It is the case for Fe-V-Al compounds for which maximum n- and p-Seebeck coefficients are found for slight shifts from perfect stoichiometry [7].

2.2. Description of the present model

Introducing disorder into the crystallographic structure modifies the structure factor ratios, hence the diffracted intensities, as they are dependent on the position and the nature of the atoms in the unit cell (see Equations (1) and (2)). As a reminder, the $L2_1$ structure is constituted of four FCC sublattices: X, Y, X′, and Z, occupied for the stoichiometric Fe_2VAl compound by Fe, V, Fe, and Al, respectively. Similar occupancy of both Fe sublattices is assumed in all cases (X = X′), meaning that V or Al atoms could not substitute on one Fe sublattice preferentially. This assumption is consistent with previous literature on Fe_2VAl-based compounds [1].

In order to be able to take into account off-stoichiometry, the probability of occupancy of the constitutive elements in the unit cell is described by nine general parameters p_i^j, which represent the atomic fraction of i atom (i = Fe, V, or Al) occupying j site (j = X, Y, or Z), similarly to Umetsu's model [19]. Equation (5) relates the p_i^j parameters, i.e. the total proportion of each atom is equal to its concentration and the sum of the proportions of each site equals 1.

$$\begin{aligned} &0.5p_i^X + 0.25p_i^Y + 0.25p_i^Z = c_i \\ &p_{Fe}^{j} + p_V^{j} + p_{Al}^{j} = 1 \end{aligned} \tag{5}$$

However, since it is assumed that $c_{Fe} + c_V + c_{Al} = 1$, only five of these equations are independent. Four free variables are thus chosen among the nine parameters for the present model: $a = p_{Fe}^{X}$, $b = p_{Fe}^{Z}$, $c = p_{Al}^{X}$, and $d = p_{Al}^{Z}$. The occupancy of the constitutive elements in the unit cell is then described as a function of these four free parameters by Equation (6).

$$\begin{array}{c} \\ Fe \\ V \\ Al \end{array} \begin{array}{c} \begin{array}{ccc} X, X' & Y & Z \end{array} \\ \begin{pmatrix} a & 4c_{Fe} - 2a - b & b \\ 1 - a - c & 4c_V - 3 + 2a + 2c + b + d & 1 - b - d \\ c & 4 - 4c_{Fe} - 4c_V - 2c - d & d \end{pmatrix} \end{array} \tag{6}$$

With this general description of the occupancy of the Fe, V, and Al atoms, one can describe any $L2_1$, $D0_3$, B2 or A2 structure for any composition. For example, Table 1 gives the values of a, b, c, and d for a stoichiometric compound with the above-mentioned structures. It is worth noting that, when dealing with off-stoichiometric compounds, it is impossible to reach the fully ordered $L2_1$ structure, even though a and d may be equal to 1 and b and c to 0.

Based on Equation (6), the structure factors can be written, from Equation (2), as a function of the probabilities of occupancy, as shown in Table 2. It highlights that (220) is a fundamental reflection independent of order, hence of a, b, c, and d. On the other hand, (111) and (200) are superlattice, order-dependent, reflections. For stoichiometric samples, with the A2 structure, both superlattice structure factors are zero. The B2 structure brings about a null (111) reflection, while the (200) structure factor is similar to the one of the $L2_1$ structure. For the $D0_3$ structure, the different superlattice reflections are present but with intensities different from the $L2_1$ structure.

Since the model takes into account anomalous scattering, X-ray atomic scattering factors f_{at} are calculated with Equation (3), hence dependent on the X-ray source (λ) and on the considered reflection (θ). More precisely, one should have written $f^{111}{}_{at}$, $f^{200}{}_{at}$, and $f^{220}{}_{at}$ for the first, second, and third lines in Table 2, respectively. f_0 depends on the radial distribution of the electron density in the atom [17]. No analytical expression exists for its estimation since it requires the calculation of several integrals (one per electronic shell). f_0 is often tabulated in the literature for given values of sinθ/λ, hence independently of the X-ray source [15,17]. Here, f_0 is interpolated following Equation (7), inferred from Cullity's table [15], and calculated for $x = \sin\theta/\lambda$ corresponding to the 2θ positions of a standard Fe_2VAl pattern. It is worth noting that Equation (7) do not have any physical meaning, except the constant term that is close to Z_{at}.

$$\begin{aligned} Fe:&\quad f_0 = 26.11 - 32.40x - 10.00x^2 \\ V:&\quad f_0 = 23.07 - 29.85x - 7.50x^2 \\ Al:&\quad f_0 = 13.05 - 23.80x + 20.00x^2 \end{aligned} \tag{7}$$

f′ and f″ values, given in Table 3, are obtained from Merritt's website [18] where the anomalous scattering coefficients are tabulated as a function of incident X-ray energy for each element of the periodic table.

The theoretical expressions of the structure factor ratios, found from Table 2, are compared to the experimental structure factor ratios, obtained from the experimental intensities for both Co and

Table 1
Values of the four probabilities of occupancy, chosen as free variables for the present model, for a stoichiometric Fe_2VAl compound presenting the different disordered structures.

	a	b	c	d
A2	1/2	1/2	1/4	1/4
B2	1	0	0	1/2
$D0_3$	2/3	0	0	1
$L2_1$	1	0	0	1

Table 2
Structure factors of various reflections for the disordered Fe_2VAl compound as a function of the probabilities of occupancy a, b, c, and d.

Reflection		$\lvert F_{hkl}\rvert^2 \sim$
(111)	S_I	$[(4c_{Fe} - 2a - 2b)f_{Fe} + (4c_V - 4 + 2a + 2b + 2c + 2d)f_V + (4 - 4c_{Fe} - 4c_V - 2c - 2d)f_{Al}]^2$
(200)	S_{II}	$[(4a - 4c_{Fe})f_{Fe} + (4 - 4c_V - 4a - 4c)f_V + (4c_{Fe} + 4c_V - 4 + 4c)f_{Al}]^2$
(220)	F	$[(4c_{Fe})f_{Fe} + (4c_V)f_V + (4 - 4c_{Fe} - 4c_V)f_{Al}]^2$

Table 3
Real and imaginary parts of the atomic scattering factors of Fe, V, and Al for Co and Cr X-ray sources [18].

Source		Fe	V	Al
Co Kα1	f′=	−3.33	−0.46	0.25
	f″=	0.49	2.68	0.33
Cr Kα1	f′=	−1.29	−4.48	0.33
	f″=	0.77	0.46	0.52

Cr sources and calculated with Equation (1). In order to quantify (dis)order, fitting by least square method is then used to find the quadruplet a, b, c, and d that gives the best fit of the experimental ratios of structure factors. It is worth noting that a, b, c, and d are imposed to lay between 0 and 1. Additional constraints are added to ensure that each probability of occupancy of Equation (6) is also between 0 and 1, e.g. $0 \leq 1 - a - c \leq 1$.

2.3. Comparison with other models

The α, β, and γ exchange parameters defined by Takamura et al. and the ordering parameters defined in the present model can be compared. Takamura's model assumes exact stoichiometry and exchanges between Fe/Al, Al/V, and Fe/V [10]. Since only pairwise exchanges are considered, it means that b and c are not independent; Equation (6) indeed showed that b and c are the probabilities of occupancy of Fe on Z sites and of Al on X sites, respectively. Assuming stoichiometry and $b = 2c$, a correspondence exists between both models: $a = 1 - \beta/2 - \gamma/2$, $b = 2c = \beta$, and $d = 1 - \alpha - \beta$. Based on present results, the $b = 2c$ assumption is not too restrictive when considering ordering since both parameters tend to be close to 0. However, this is not the case for off-stoichiometric samples heat-treated in such a way to induce disordering.

On the other hand, Umetsu et al. [19] considered four independent atomic fractions (or probabilities of occupancy), similarly to the present model, so that it is also not limited to pairwise exchanges. However, in addition to the exact stoichiometry, the assumption that $b = c = 0$ was then imposed. It is thus impossible to describe the disordered A2 structure and to discuss disordering phenomena based on Umetsu's model.

3. Experimental work

3.1. Materials and methods

The Fe_2VAl samples were processed by casting appropriate amounts of ferro-vanadium (81 wt% of V) with additional pure iron and aluminium. Induction heating was used to melt the base materials. Bulk samples were then ground in an annular steel grinder for 40 s. Heat-treatments were applied on ground samples sealed in evacuated quartz capsules backfilled with Ar.

XRD was performed on powdered samples after grinding and after additional heat-treatments. Based on Fig. 2, Co Kα1 and Cr Kα1 sources were selected to perform X-ray diffraction, taking into account anomalous scattering on Fe_2VAl samples. (220) being a fundamental reflection independent of order, as shown on Table 2, each diffraction pattern has been normalised with respect to the integrated intensity of its (220) peak before analysis since the ratios of structure factor are used for the quantitative model (see Section 2) and not the value of each structure factor independently.

Neutron diffraction experiments were performed on similar samples at the Paul Scherrer Institut (The Swiss Spallation Neutron Source and High-Resolution Powder Diffractometer for Thermal Neutrons). Neutron diffractograms were analysed by Rietveld analysis in order to determine the proportions of atomic exchanges α, β, and γ, as defined by Takamura [10]. The probabilities of occupancy are then calculated based on Equation (6) to be compared to XRD results.

Differential scanning calorimetry was carried out on a ground sample at a rate of 10 K min^{-1} under He in order to determine potential transition temperatures. Fig. 3 shows that potential transitions occur at different temperatures during heating: $T_1 = 1390$ K and $T_2 = 1520$ K. Maier et al. [21] recently published DTA results with similar transitions at slightly lower temperatures (1353 and 1463 K, respectively). Present ordering heat-treatments were thus performed at 1273 K, hence before T_1, also in agreement with the literature [4,7]. On the other hand, temperatures between T_1 and T_2 but also after T_2 were selected for the disordering heat-treatments, i.e. 1423 K and 1573 K, respectively.

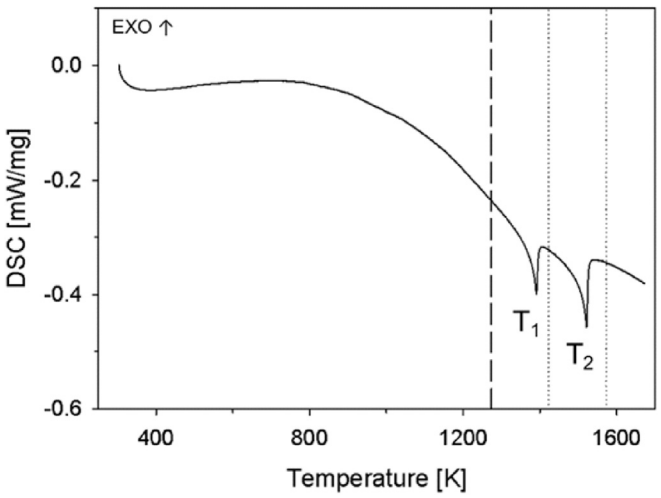

Fig. 3. Differential scanning calorimetry (DSC) curve for a Fe_2VAl ground sample (heating rate = 10 K/min). The transition temperatures are highlighted by T_1 and T_2. The ordering and disordering heat-treatments temperatures are shown by the dashed and dotted lines, respectively.

Finally, some electron backscattered diffraction (EBSD) analyses were carried out on powders after different processing conditions.

3.2. Experimental XRD results

Fig. 4 shows the typical superlattice reflections in the case of a cast and ground Fe_2VAl sample as well as after additional ordering heat-treatments. The diffraction peaks representative of the $L2_1$ structure, e.g. (111), are easily identified with an increasing intensity already after the heating stage up to 1273 K. The integrated intensity of the (111) peak hardly increases with the addition of a 1 h-plateau at 1273 K.

On the other hand, it seems that the (200) peak intensity slightly increases while heating up to 1273 K. It could be the sign that the samples are in the B2 state before the ordering treatment, since $|F_{200}|^2/|F_{220}|^2$ is similar for B2 and $L2_1$ (Tables 1 and 2).

The disordering heat-treatments at 1423 and 1573 K, followed by water quenching, lead to a decrease of the normalised intensity of the (111) peak, while the (200) peak stays roughly constant. Qualitatively, these samples appear still more ordered than the ground samples.

The full width at half-maximum (FWHM) of the fundamental (220) diffraction peak is another interesting parameter to analyse. The (220) FWHM is divided by a factor of 2 after 1 h of heat-treatment at 1273 K. The same trend is qualitatively observed for the superlattice diffraction peaks (Fig. 4). The narrowing of the peaks is the sign of a decrease of defects density such as dislocations. Indeed, even though Fe_2VAl-related compounds are brittle enough to be ground, the inverse pole figure (IPF) map of Fig. 5(a) shows that large gradients of crystal orientations related to some plasticity can be observed. Furthermore, very interestingly, subsequent heat-treatment at 1273 K leads to recrystallization with the nucleation and growth of new grains, as shown on Fig. 5(b–d). This fully agrees with the evolution of the FWHM observed on Fig. 4 [16].

Finally, Fig. 6 compares the diffractograms of a sample held at 1273 K for 2 h and then measured with either a Co or a Cr source. It highlights the major influence of anomalous scattering for the Fe_2VAl-based compounds, as described in Section 1 and Fig. 2. Indeed, the use of the Cr source results in a decrease of the (111) reflection, while the relative intensity of the (200) peak rises.

4. Discussion

Based on the work of Bragg and Williams [22,23], ordering parameter S is used in the present paper to discuss the ordering and disordering phenomena. It is defined by Equation (8), where p is the actual probability of occupancy of the constitutive elements in the unit cell, while $p_{disordered}$ and $p_{ordered}$ stand for the completely disordered (A2) and ordered ($L2_1$) structures, respectively.

$$S = \frac{p - p_{disordered}}{p_{ordered} - p_{disordered}} \tag{8}$$

Generally speaking, the ordering parameters, also referred to as degrees of order in the literature, compare the actual probability of occupancy p with the values for the completely disordered and ordered structures. In the present work, four ordering parameters S_a, S_b, S_c, and S_d are calculated, one for each of the probabilities of occupancy obtained from the model: p = a, b, c, or d (see Section 2).

The definition of Equation (8) is very convenient for stoichiometric compounds, as it is mostly assumed in the literature [19,22,23]. However, since the present work aims at developing a model able to take account of off-stoichiometry in the analysis of (dis)ordering phenomena, some hypotheses are required to specify $p_{disordered}$ and $p_{ordered}$ (summarised in Table 4). On the one hand, it is straightforward to state that the probability of occupancy for a completely disordered structure is equal to the quantity of the considered element in the alloy. In a disordered structure, each position in the unit cell is statistically occupied by c_{Fe} Fe atoms, c_V V atoms, and c_{Al} Al atoms when c_X is the atomic concentration of element X. On the other hand, $p_{ordered}$ is assessed for the perfectly $L2_1$ ordered structure, hence for the strict 2-1-1 stoichiometry (same values as in Table 1). Indeed, defining $p_{ordered}$ for off-stoichiometric compounds is tricky and subjective, but it also may lead to ordering parameters larger than 1.

Similarly to Table 1, Table 5 gives examples of the four ordering parameters for stoichiometric Fe_2VAl compounds from a disordered structure (all S = 0) to an ordered structure (all S = 1).

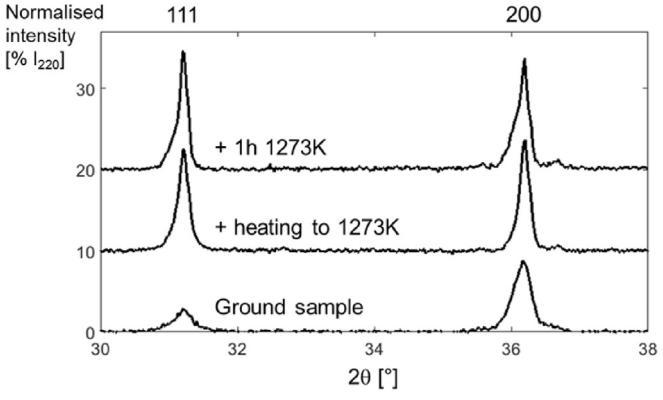

Fig. 4. X-ray diffractograms (Co Kα1 source) of the base cast and ground sample, after heating to 1273 K, and with an ordering heat-treatment at 1273 K for 1 h. Zoom around the (111) and (200) superlattice reflections.

4.1. Quantitative analysis of the X-ray diffraction results

The model presented in Section 2.2 has been applied to various experimental Co and Cr XRD results to obtain quantitative analysis of the (dis)ordering phenomena.

Fig. 7 presents the evolution of S_b and S_d with respect to the holding time at the ordering temperature (1273 K), while S_a and S_c remain close to 1 in any case. With $S_d = 0.48$, the base cast and ground sample has a significant proportion of V/Al exchanges (B2 structure gives $S_d = 1/3$, see Table 5). From Fig. 7, it is highlighted that heat-treating at 1273 K is very effective to generate ordered phases starting from ground samples. After heating up to 1273 K (with a heating rate of 400 K min^{-1} followed by air-quenching), the S_d parameter already rises to 0.8, meaning that the proportion of Al located on the right Z sites has rapidly increased by a factor 2. The S_d parameter then gradually increases with a value of 0.95 after 2 h at 1273 K. Fig. 5(b–d) highlighted that recrystallization is also initiated by the applied heat treatment, with a kinetics similar to the observed evolution of the order parameters. Based on these results, it appears that the cast and ground samples present a structure closer to B2, while heat-treatments at 1273 K substantially promotes $L2_1$ ordering and recrystallization which is based on a complete reconstruction of the lattice. These two phenomena thus seem concomitant.

Nishino et al. [4,7,11] suggested ordering heat-treatments in two steps for Fe_2VAl-based samples, 1 h at 1273 K followed by 4 h at 673 K. The two-steps treatment has been applied and compared with samples heat-treated at 1273 K for 1 h only. The red star symbols on Fig. 7 show that the S_b and S_d parameters for the two heat-treatments are similar, thus highlighting the major efficiency of the ordering stage at 1273 K.

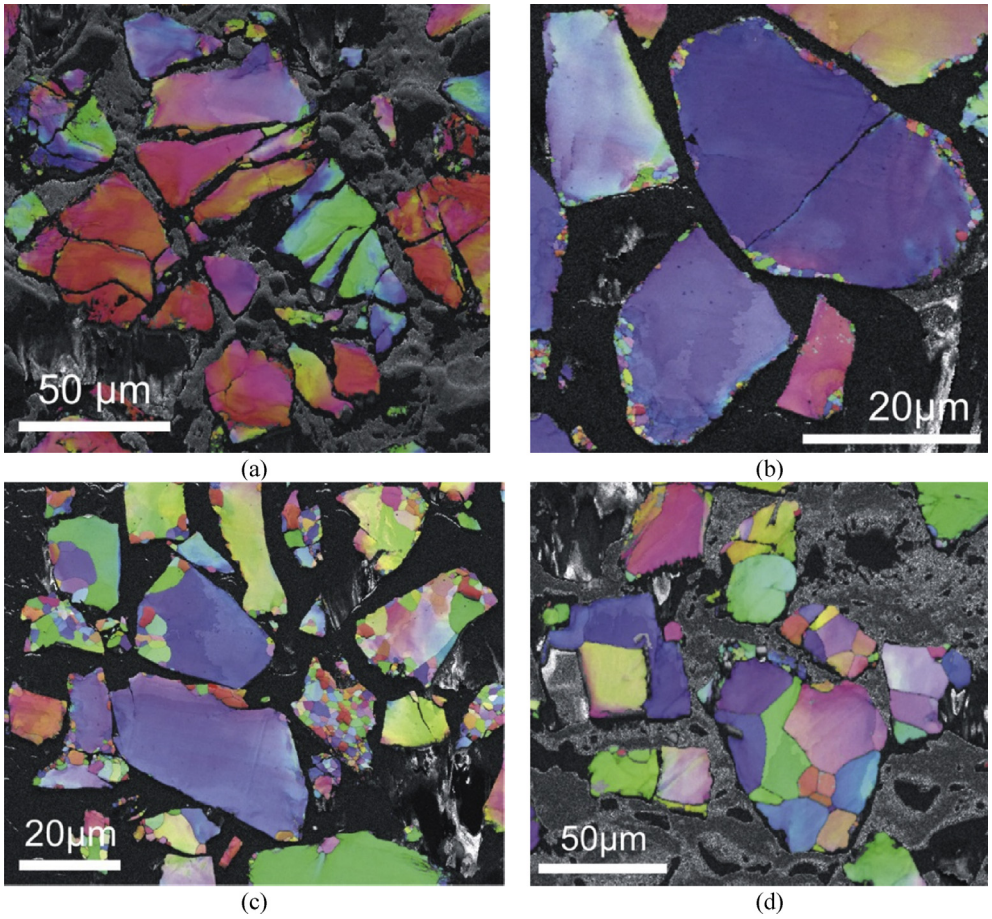

Fig. 5. EBSD maps of the base cast and ground powder (a) and of samples heat treated at 1273 K for 0 min (heating stage up to 1273 K and no hold) (b), 5 min (c) and 6 h (d). While the ground powder appears plastically deformed, recrystallization seems to start in the early stage of the heat treatment at 1273 K as shown by the new grains appearing and consuming the deformed grains.

In agreement with the DSC curve of Fig. 3, disordering potentially occurs above 1390 K. Heat-treatments at 1423 K or 1573 K, followed by water quenching, were thus applied on ground samples. After 5 min at 1423 K, S_a, S_b and S_c are still equal to 1 and the decrease of S_d to 0.86 shows the beginning of the formation of B2. The heat-treatment of 2 min at 1573 K involves limited B2 disordering with $S_d = 0.76$, still higher than its value after grinding ($S_d = 0.48$). S_a and S_c values remain at 1, while S_b decreases slightly at 0.96, reflecting that no A2 structure was formed after water quenching from 1573 K (see Table 5). An additional sample was also fabricated by melt-spinning, a solidification process with very high cooling rate directly from the melt, and it does not exhibit the A2 structure but the value of S_d is much smaller ($S_d = 0.43$). As suggested in the literature [24,25], it appears that the disordered A2 structure is not easily retained at room temperature since B2 ordering occurs at very high rate.

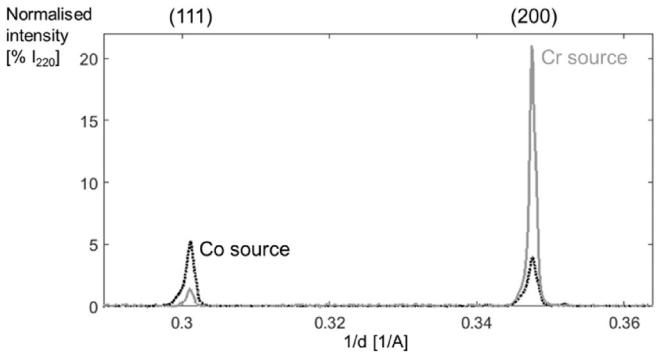

Fig. 6. Comparison of the Co (dotted black) and Cr (full grey) X-ray diffractograms of the same Fe_2VAl sample heat-treated at 1273 K for 2 h.

Table 4
$p_{disordered}$ and $p_{ordered}$ parameters of Equation (8) specified for each ordering parameter S.

	S_a	S_b	S_c	S_d
$p_{disordered}$ =	c_{Fe}	c_{Fe}	c_{Al}	c_{Al}
$p_{ordered}$ =	1	0	0	1

4.2. Comparison of the model with neutron diffraction results

Some neutron diffraction experiments were also performed on

Table 5
Values of the four ordering parameters for a stoichiometric Fe_2VAl compound with various (dis)ordered structures.

	S_a	S_b	S_c	S_d
A2	0	0	0	0
B2	1	1	1	1/3
DO_3	1/3	1	1	1
$L2_1$	1	1	1	1

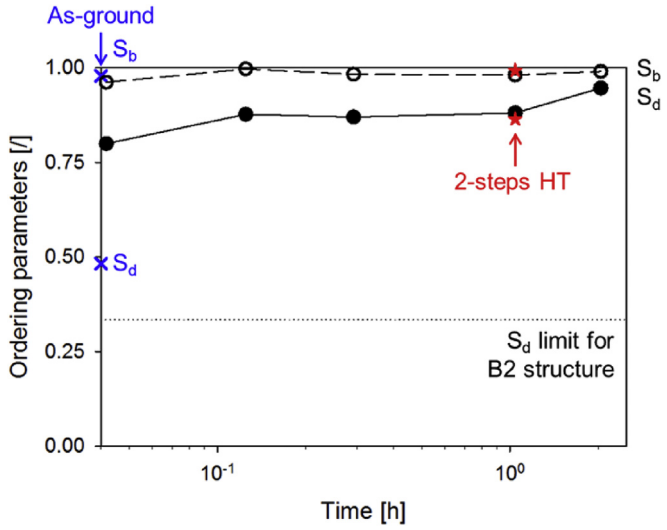

Fig. 7. Evolution of the S_b (open circles) and S_d (full circles) parameters as a function of the duration of the ordering heat-treatment at 1273 K. The S_a and S_c parameters are not shown since they remain constant very close to 1. The blue crosses represent the initial ground sample and the red stars correspond to the two-steps heat-treatment: 1 h at 1273 K followed by 4 h at 673 K. No significant difference is observed between both heat-treatments. The dotted line is the 0.33 limit corresponding to the B2 structure. (For interpretation of the references to colour in this figure legend, the reader is referred to the web version of this article.)

cast, ground, and heat-treated samples. As stated by Umetsu et al. [19] and Maksimov et al. [26], even though it is much less available, neutron diffraction could be an alternative technique to observe the superstructure of $Fe_{2+x}V_{1-x}Al$ alloys since Fe, V, and Al present largely different neutron scattering lengths.

The cast and ground sample presents the (200) superlattice reflection, typical of the B2 phase. After an ordering heat-treatment of 6 h at 1273 K, the superlattice reflections corresponding to $L2_1$ clearly appear, e.g. (111).

Fig. 8 presents the evolution of the order parameters, estimated from neutron diffraction measurements, as a function of the holding time at 1273 K. An important increase of S_d is observed after 2 h at 1273 K, while no further evolution is then observed up

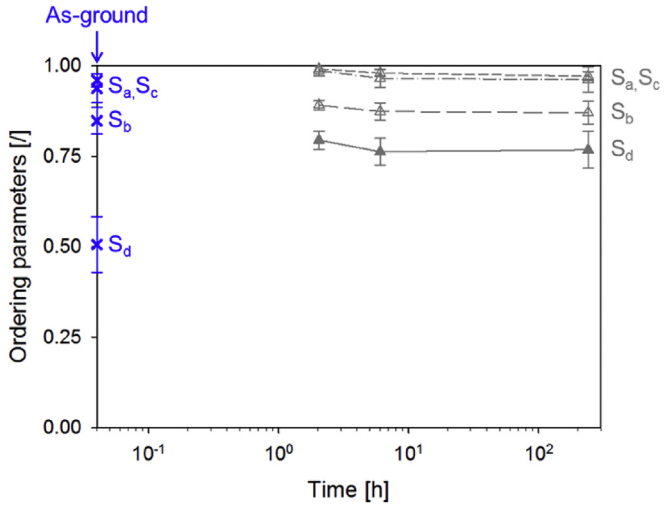

Fig. 8. Evolution of the ordering parameters, calculated based on neutron diffraction results, as a function of the holding time at 1273 K. The blue crosses represent the initial ground sample. (For interpretation of the references to colour in this figure legend, the reader is referred to the web version of this article.)

to 10 days of heat-treatment. S_a and S_c parameters remain close to 1 in these experiments, while S_b does not evolve significantly and fluctuates around 0.87.

It is worth comparing the evolution of the S_d parameter calculated from the Co and Cr XRD (present model) and from neutron diffraction analysed by Rietveld analysis. However, an inherent difference between both strategies results from the Rietveld analysis of neutron measurements that is limited to pairwise exchanges applying to the ordered structure. Since off-stoichiometry is considered here, the "most ordered structure" depends on the actual composition of the sample. While $S_{d,max}$ is equal to 1 in the present model (when $d = d_{ordered} = 1$), $S_{d,max}$ is limited to 0.92 in the "most ordered case" of the neutron analysis, due to the actual off-stoichiometry of the analysed samples. The comparison of XRD and neutron results is then based on the difference between $S_{d,max}$ and the calculated S_d parameter. Fig. 9 analyses the evolution of $S_{d,max}$-S_d with holding time at 1273 K. It shows that the present model combining Co and Cr XRD and taking into account anomalous scattering catches pretty well the evolution of the S_d parameter from the B2 to the $L2_1$ structures, similarly to neutron diffraction. XRD and neutron results match also for the other ordering parameters even though the comparison is not presented since the differences with S_{max} are very small.

4.3. Scenario of (dis)ordering of Fe_2VAl compounds

From the analysis of the diffraction and DSC results, the following scenario can be proposed for the ordering/disordering of Fe_2VAl-based.

The cast and ground Fe_2VAl-based samples present significant B2 disorder. Indeed, both X-ray (Co and Cr sources - Fig. 7) and neutron diffraction (Fig. 8) bring values of S_d close to 0.5. It means that almost 40% of the V and Al atoms present antisite locations. This first conclusion matches up with recent results published by Maier et al. [21] who identified B2 disorder after moderate mechanical stress, such as hand grinding.

Heat-treatments at 1273 K performed on powdered samples are highly efficient to increase the degree of $L2_1$ order. The (111)

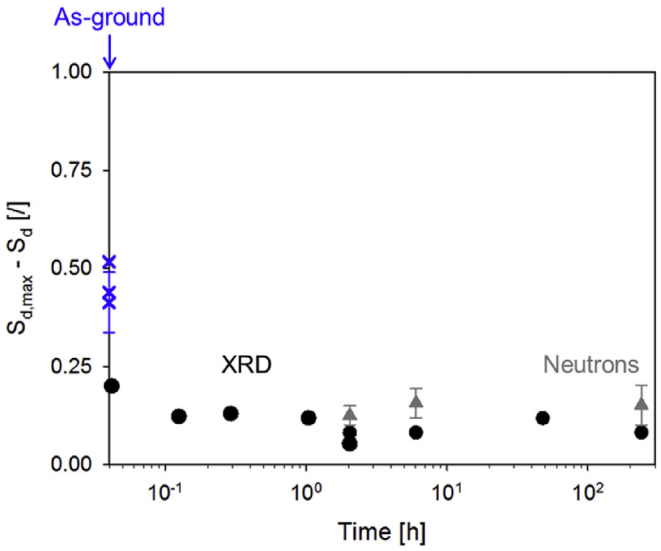

Fig. 9. Comparison of the evolution of $S_{d,max}$-S_d calculated from XRD with the present model (black circles) or from neutron diffraction experiments with a Rietveld refinement analysis (grey triangles). The blue crosses represent initial ground samples. (For interpretation of the references to colour in this figure legend, the reader is referred to the web version of this article.)

superlattice reflection is greatly enhanced already after the heating step up to 1273 K. S_d continuously increases when extending the heat-treatment (Fig. 7). While S_b remains close to 0.98, the S_a and S_c parameters are equal to 1, whatever the duration of the 1273 K heat-treatment is. It was shown that recrystallization also occurs during this heat treatment. It is assumed that both phenomena interact with each other in a way that would worth being further investigated.

The T1 peak around 1390 K on Fig. 3 is associated with the appearance of the B2 phase. Indeed, the present model suggests that the sample heat-treated at 1423 K presents V/Al antisite defects, but still in a low proportion (around 10%). In addition, some hot-compression tests [27] highlighted a significant transition in the mechanical behaviour of Fe_2VAl-based compounds between 1373 K and 1473 K, which could be related to the long-range order (as suggested by Nishino et al. [4]). Finally, this transition temperature of 1390 K perfectly fits with the temperature suggested by Nishino et al. for the $D0_3$-B2 transition of stoichiometric Fe_2VAl compound [4] and rather well with results from Maier et al. [21] or Ferreiros et al. [24].

The T2 peak around 1520 K on Fig. 3 may correspond to the onset of A2 disordering. Experimentally, no sample was successfully retained in the A2 state at room temperature, neither by water quenching or melt-spinning. The B2 to A2 transition temperature suggested by the present paper is slightly lower than the one highlighted by Maier et al. using high-temperature neutron diffraction [21].

5. Conclusions

The present paper summarises the analysis carried out to gain understanding of the crystal structures of Heusler Fe_2VAl-based compounds and the related ordering transformations. Identifying the corresponding phases required to successfully combine several characterisation techniques (DSC, X-ray anomalous diffraction, neutron diffraction and EBSD). A model has been developed to quantify the ordering parameters $S_{a,b,c,d}$ of off-stoichiometric Fe_2VAl-based compounds from the combination of Co and Cr XRD results. By choosing appropriate X-ray sources, this model could easily be generalised to other ternary structures, such as other Heusler compounds which are mostly based on chemical elements with close atomic numbers. Based on experimental XRD measurements, the developed model gave ordering parameters comparable to those obtained from a Rietveld refinement analysis of neutron diffraction results. It brought the conclusion that heat-treatments at 1273 K on ground samples are highly efficient for B2-to-$L2_1$ ordering. The onset of B2 and A2 disordering were also highlighted around 1390 K and 1520 K, respectively. Further developments would focus on a deeper analysis of the relationship between ordering and recrystallization. Furthermore, it would be worth checking the actual presence of the A2 state owing to high temperature in situ diffraction.

Acknowledgments

The authors acknowledge the financial support from the Interuniversity Attraction Poles Program from the Belgian State through the Belgian Policy agency; contract IAP7/21 "INTEMATE". The authors acknowledge S. Godet and T. Segato from ULB for the DSC measurements.

References

[1] T. Graf, C. Felser, S.S.P. Parkin, Simple rules for the understanding of Heusler compounds, Prog. Solid State Chem. 39 (2011) 1–50.
[2] T. Graf, C. Felser, Heusler compounds at a glance, in: C. Fesler, G.H. Fecher (Eds.), Spintronics – From Materials to Devices, Springer, 2013, pp. 1–14.
[3] B. Balke, G.H. Fecher, C. Felser, New Heusler compounds and their properties, in: C. Fesler, G.H. Fecher (Eds.), Spintronics – From Materials to Devices, Springer, 2013, pp. 15–43.
[4] Y. Nishino, Y. Makino, Effect of vanadium substitution on strength properties of Fe_3Al-based alloys, Mater. Sci. Eng. A (2001) 368–371, 319-321.
[5] M. Mikami, A. Matsumoto, K. Kobayashi, Synthesis and thermoelectric properties of microstructural Heusler Fe_2VAl alloy, J. Alloy. Compd. 461 (2008) 423–426.
[6] Y. Nishino, Development of thermoelectric materials based on Fe_2VAl Heusler compound for energy harvesting applications, Mater. Sci. Eng. 18 (2011), 142001.
[7] H. Miyazaki, S. Tanaka, N. Ide, K. Soda, Y. Nishino, Thermoelectric properties of Heusler-type off-stoichiometric $Fe_2V_{1+x}Al_{1-x}$ alloys, Mater. Res. Express 1 (2014), 015901.
[8] M. Mikami, M. Inukai, H. Miyazaki, Y. Nishino, Effect of off-stoichiometry on the thermoelectric properties of Heusler-type Fe_2VAl sintered alloys, J. Electron. Mater. 45 (2016) 1284–1289.
[9] D.I. Bilc, P. Ghosez, Electronic and thermoelectric properties of Fe_2VAl: the role of defects and disorder, Phys. Rev. B 83 (2011), 205204.
[10] Y. Takamura, R. Nakane, S. Sugahara, Quantitative analysis of atomic disorders in full-Heusler Co_2FeSi alloy thin films using X-ray diffraction with Co-Kalpha and Cu-Kalpha sources, J. Appl. Phys. 107 (2010), 09B111.
[11] M. Kato, Y. Nishino, U. Mizutani, S. Asano, Electronic, magnetic and transport properties of (Fe1−xVx)3Al alloys, J. Phys. Condens. Mater. 12 (2000) 1769–1779.
[12] Y. Feng, J.Y. Rhee, T.A. Wiener, D.W. Lynch, B.E. Hubbard, A.J. Sievers, D.L. Schlagel, T.A. Lograsso, L.L. Miller, Physical properties of Heusler-like Fe_2VAl, Phys. Rev. B 63 (2001), 165109.
[13] J.I. Langford, D. Louër, Powder diffraction, Rep. Prog. Phys. 59 (1996) 131–234.
[14] A. Bradley, J. Rodgers, The crystal structure of the Heusler alloys, P. R. Soc. Lond. A 144 (1934) 340–359.
[15] B.D. Cullity, S.R. Stock, Elements of X-ray Diffraction, third ed., Prentice-Hall, Upper Saddle River, 2001.
[16] P. Gravereau, Introduction à la pratique de la diffraction des rayons X par les poudres, 3ème cycle, Diffraction des rayons X par les poudres, Univ. Bordx. 1 (2011) 209.
[17] B.E. Warren, X-ray Diffraction, Addison-Wesley Pub. Co, 1969.
[18] E.A. Merritt, X-ray Anomalous Scattering, 2012. http://skuld.bmsc.washington.edu/scatter/. (Accessed 7 July 2015).
[19] R. Umetsu, K. Kobayashi, R. Kainuma, Y. Yamaguchi, K. Ohoyama, A. Sakuma, K. Ishida, Powder neutron diffraction studies for the $L2_1$ phase of Co_2YGa (Y = Ti, V, Cr, Mn and Fe) Heusler alloys, J. Alloy. Compd. 499 (2010) 1–6.
[20] V. Pomjakushin, HRPT: High-resolution Powder Diffractometer for Thermal Neutrons, 2013. http://sinq.web.psi.ch/sinq/instr/hrpt/index.html. (Accessed 7 July 2015).
[21] S. Maier, S. Denis, A. Adam, J.-C. Crivello, J.-M. Joubert, E. Alleno, Order-disorder transitions in the Fe_2VAl Heusler alloy, Acta Mater. 121 (2016) 126–136.
[22] W. Bragg, E. Williams, The effect of thermal agitation on atomic arrangement in alloys, P. R. Soc. Lond. A 145 (1934) 699–730.
[23] W. Bragg, E. Williams, The effect of thermal agitation on atomic arrangement in alloys II, P. R. Soc. Lond. A 151 (1935) 540–566.
[24] P.A. Ferreiros, P.R. Alonso, P.H. Gargano, P.B. Bozzano, H.E. Troiani, A. Baruj, G.H. Rubiolo, Characterization of microstructures and age hardening of $Fe_{1-2x}Al_xV_x$ alloys, Intermetallics 50 (2014) 65–78.
[25] M. Marcinkowski, N. Brown, Theory and direct observation of dislocations in the Fe_3Al superlattices, Acta Metall. Mater. 9 (1961) 764–786.
[26] I. Maksimov, D. Baabe, H.H. Klauss, F.J. Litterst, R. Feyerherm, D.M. Tobbens, A. Matsushita, S. Sullow, Structure and magnetic order in $Fe_{2+x}V_{1-x}Al$, J. Phys. Condens. Mater. 13 (2001) 5487–5501.
[27] C. van der Rest, P.J. Jacques, Unpublished Results.